Simultaneous Stabilization of Stall and Surge via Axisymmetric Air Injection*

Simon Yeung
cxy@indra.caltech.edu

Richard M. Murray
murray@indra.caltech.edu

Division of Engineering and Applied Science
California Institute of Technology
Pasadena, California 91125

Submitted, *35th AIAA/ASME/SAE/ASEE Joint Propulsion Conference*

September 25, 1998

Abstract

Simultaneous control of stall and surge has been achieved on a low speed, single stage, axial compressor using axisymmetric air injection. Two cases with different injector back pressure are studied. Control is achieved for one of the cases, but is not achieved for the lower authority case. This is consistent with previous results for control of stall only with axisymmetric air injection without a plenum attached. A simulated proportional injection mechanism is implemented and control is also achieved.

Nomenclature

B, l_c, m, a	compressor model parameters[9]
A	amplitude of first Fourier mode
γ	throttle coefficient $\Phi_T(\psi) = \gamma\sqrt{\psi}$
J	$= A^2$
J_{thresh}	threshold on J
K	gain used for stall control
$\hat{K}$	gain used for surge control
$K_{\min}$	minimum gain required for elimination of hysteresis loop for stall control
ϕ	nondimensionalized velocity
$\Phi_T(\psi)$	throttle characteristic $= \gamma\sqrt{\psi}$
ψ	nondimensionalized pressure rise
$\Psi_c(\phi)$	compressor characteristic
$\Psi_{c,\text{nom}}(\phi)$	nominal compressor characteristic
$\Psi_{c,\text{air}}(\phi)$	contribution to compressor characteristic via air injection
x_0	x at peak of compressor characteristic

1. Introduction

Rotating stall and surge are two examples of instabilities experienced by axial flow compressors in gas turbine engines. Stall is often irrecoverable due to the presence of hysteresis loop, in which case a shutdown and restart of the entire engine is in order. The engine can also experience significantly reduced or even reverse flow in the presence of surge, which is detrimental to combustion and the flight process.

Air injection has been proposed for control of rotating stall. Various researchers including Day,[4] Behnken,[1] D'Andrea et al.,[3] Gysling et al.,[7] Weigl,[11] Weigl et al.,[12] and Freeman et al.[6] have reported control results. In particular, Behnken,[1] Freeman et al.,[6] and Weigl[11] demonstrate control of stall using axisymmetric air injection via slightly different implementations. The combined control of rotating stall with a non-axisymmetric pulsed air injection controller and surge with a bleed valve controller has also been achieved by Behnken et al.[2]

Simultaneous stabilization of stall and surge with axisymmetric air injection however, has not been explored. If successful, new possibilities such as various combinations of actuation mechanisms for control of compressor instabilities will be created. Comparison and trade-off studies for various actuation mechanisms can then be performed. Also, with a multi-block representation of the compressor where actuation is possible for each block, the issue of actuator allocation can also be addressed and formulated.

The purpose of this paper is to outline the results of control of stall and surge using axisymmetric air injection. The theoretical justification for stabilization of stall and surge is presented in Section 2. The experimental setup used is described in Section 3. Results of the implementations are presented and

*Funding for this research was provided in part by AFOSR grant F49620-95-1-0409.

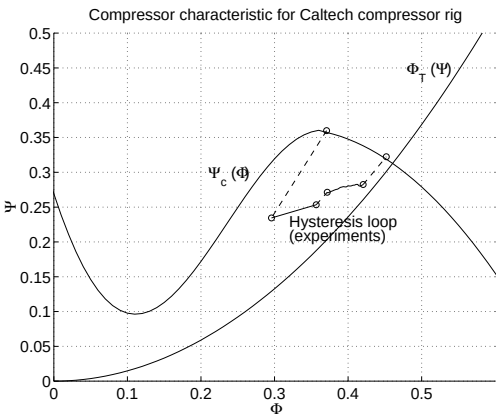

Figure. 1: Typical compressor characteristic and stalled operation.

discussed in Section 4. The paper then ends with some conclusions in Section 5.

2. Theory

In this section the Moore-Greitzer model[9] for compression systems is reviewed. Control of stall and surge is then outlined.

2.1. Basic model

By taking a simplified view of a compression system, Moore and Greitzer[9] arrive to a low order model that exhibits stall and surge. The model is a PDE describing the unsteady axial velocity and total-to-static pressure rise across the system. Fourier modes are used to decompose the stall cell and Galerkin projection is used to arrive to ODEs. The model with a one mode truncation consists of three ordinary differential equations describing the evolution of the axial velocity, pressure rise, and the square of the amplitude of the first Fourier mode:

$$\begin{aligned}\dot{\phi} &= \frac{1}{l_c}(\Psi_c(\phi) - \psi + \frac{J}{4}\frac{\partial^2\Psi_c(\phi)}{\partial\phi^2}),\\ \dot{\psi} &= \frac{1}{4l_cB^2}(\phi - \Phi_T(\psi)),\\ \dot{J} &= \frac{2a}{1+ma}J(\frac{\partial\Psi_c(\phi)}{\partial\phi} + \frac{J}{8}\frac{\partial^3\Psi_c(\phi)}{\partial\phi^3}).\end{aligned} \quad (1)$$

Figure 1 shows an example of a compressor characteristic $\Psi_c(\phi)$ and a hysteresis loop associated with rotating stall obtained experimentally.

One can find a number of bifurcations in the set of equations described by (1). Details can be found in

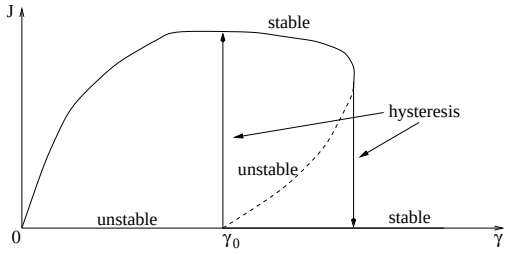

Figure. 2: Transcritical bifurcation in γ-J plane.

McCaughan.[8] Stall appearing as a subcritical transcritical while surge as a Hopf bifurcation are the dominant features in low and high values of B respectively. Figure 2 shows a picture of the transcritical stall bifurcation.

2.2. Low B

For the stall part, we first investigate linear stability. Axisymmetric air injection can be modeled as a shift of the compressor characteristic. The control law using axisymmetric air injection is modeled as a shift in the compressor characteristic with a feedback on J given by the following.

$$\Psi_c(\phi) = \Psi_{c,\mathrm{nom}}(\phi) + KJ\Psi_{c,\mathrm{air}}(\phi) \quad (2)$$

where K is the gain. Linearization of the closed-loop $\dot{J}$ equation at and to the left of the peak of $\Psi_{c,\mathrm{nom}}$ about $J = 0$ gives $\frac{d}{dt}(\delta J) = 0$ at and > 0 to the left of the peak, implying that the stall-free solution of the closed-loop system is asymptotically stable at the peak and unstable to the left of the peak.

Next we show through a bifurcation diagram that a shift in the compressor characteristic leads to elimination of the hysteresis loop. To illustrate, 3rd order polynomials are used to model a nominal compressor characteristic $\Psi_{c,\mathrm{nom}} = \sum_{i=0}^{3} a_i\phi^i$ and the addition $\Psi_{c,\mathrm{air}} = \sum_{i=0}^{3} b_i\phi^i$ due to the air injection. The new equilibria can be found by solving for the steady state solution (ϕ, ψ, J) to the governing equations. The minimum gain K required to eliminate the hysteresis loop can be found by computing the slope $\frac{dJ}{d\gamma}|_{\gamma=\gamma_0}$ and requiring $\frac{dJ}{d\gamma}|_{\gamma=\gamma_0} < 0$. The resulting expression for K_{min} is presented here without the algebra:

$$K_{\mathrm{min}} = -\frac{\frac{\gamma_0^2}{4}{\Psi'_{c,\mathrm{nom}}}^2(\phi_0) + \frac{\phi_0}{4}\Psi'''_{c,\mathrm{nom}}(\phi_0)}{2\phi_0{\Psi'}_{c,\mathrm{air}}(\phi_0) + \gamma_0^2\Psi_{c,\mathrm{air}}\Psi''_{c,\mathrm{nom}}(\phi_0)}. \quad (3)$$

Figure 3 shows sample nominal and shifted compressor characteristics and the location of the new equilibria with $B = 0.1$ and $K = 18$, both in the (ϕ, ψ) plane and the (γ, J) plane.

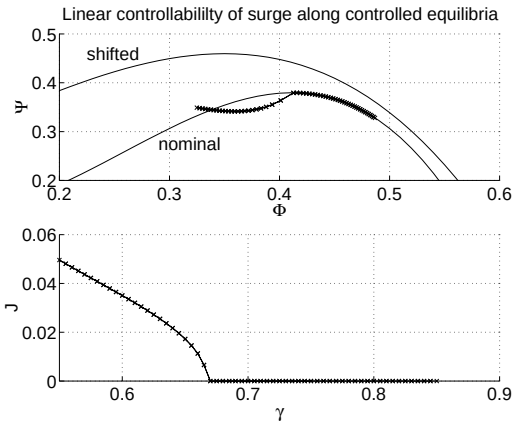

Figure. 3: Nominal, shifted compressor characteristics, and the new equilibria with axisymmetric air injection controller for stall.

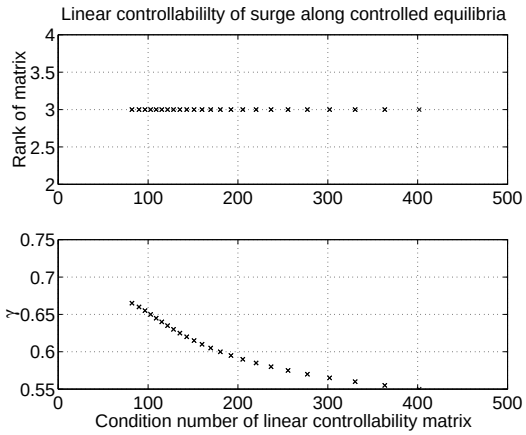

Figure. 4: Numerical evaluation of the rank of controllability matrix along equilibria of the system with axisymmetric air injection control for stall.

2.3. High B

For the surge part, we show by linearization along the controlled equilibria that the surge equations (ϕ and $\dot{\psi}$) are controllable. The linearization of eq (1) with (2) takes the form $\frac{d}{dt}(\delta x) = \hat{A}x + \hat{B}u$ where $x = (\phi, \psi, J)$, $\hat{A} = \begin{bmatrix} A_1 & A_2 & A_3 \end{bmatrix}_{\text{eq}}^{\text{T}}$, $\hat{B} = \begin{bmatrix} 1 & 0 & 1 \end{bmatrix}^{\text{T}}$, and

$$A_1 = \begin{bmatrix} \frac{\Psi'_{c,\text{nom}} + KJ\Psi'_{c,\text{air}} + \frac{J}{4}(\Psi'''_{c,\text{nom}} + KJ\Psi'''_{c,\text{air}})}{l_c} \\ \frac{-1}{l_c} \\ \frac{K\Psi_{c,\text{air}} + \frac{\Psi''_{c,\text{nom}}}{4} + \frac{KJ\Psi''_{c,\text{air}}}{2}}{l_c} \end{bmatrix}^{\text{T}},$$

$$A_2 = \begin{bmatrix} \frac{1}{4l_cB^2} & \frac{-\gamma}{8\sqrt{\psi}l_cB^2} & 0 \end{bmatrix},$$

$$A_3 = \begin{bmatrix} A_{31} & 0 & A_{33} \end{bmatrix},$$

$$A_{31} = \frac{2aJ(\Psi''_{c,\text{nom}} + KJ\Psi''_{c,\text{air}})}{1+ma},$$

$$A_{33} = \frac{2a(\Psi'_{c,\text{nom}} + KJ\Psi'_{c,\text{air}})}{1+ma} + \frac{aJ(\Psi'''_{c,\text{nom}} + KJ\Psi'''_{c,\text{air}})}{4(1+ma)} + \frac{2aJ(K\Psi'_{c,\text{air}} + \frac{\Psi'''_{c,\text{nom}}}{4} + \frac{KJ\Psi'''_{c,\text{air}}}{4})}{1+ma}.$$

A numerical evaluation of the rank of the matrix $[\hat{B}, \hat{A}\hat{B}, \hat{A}^2\hat{B}]$, for the values of γ that the controlled stall equilibria exist, shows that the matrix has rank 3 for the range of flow of interest, implying controllability (Figure 4).

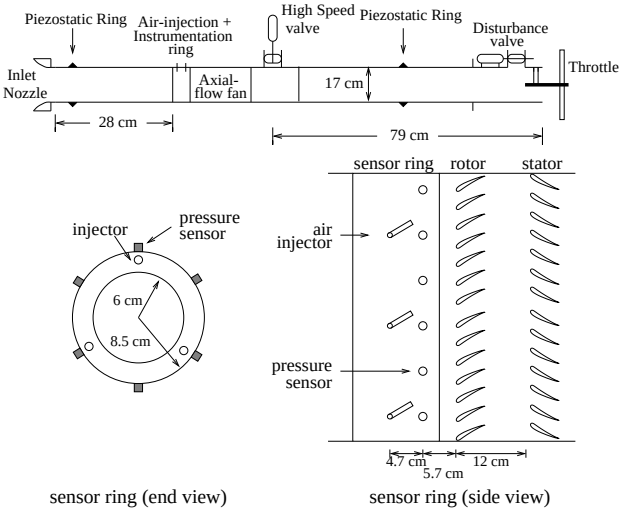

Figure. 5: Experimental setup at Caltech.

3. Experiment

Figure 5 shows the stall configuration of the experimental setup at Caltech and Table 1 the relevant parameters for the rig. Readers are referred to Yeung and Murray[13] for a more detailed description. A 4'x4'x4' plenum can be attached at the exit of the compressor to allow combined stall and surge. The plenum is attached only for the surge and combined stall-surge control experiments.

There are three air injectors with approximately 200 Hz bandwidth on the Caltech rig. At 50% duty cycle and 60 psig injector back pressure, each injector adds approximately 1.7% mass, 2.4% momentum, and 1.3% energy to the system relative to operation at the peak of the compressor characteristic.

Rig parameters	
rotor radius	8.5 cm
sensor-rotor dist.	5.7 cm
rotor-stator dist.	12 cm
rotor / stall / surge freq.	100 / 65 / 1.7 Hz
stall growth	about 30 msec

Sensor/Actuator characteristics	
Hotwire anemometer	14 cm upstream of rotor
Pressure transducers	1000 Hz BW
Binary air injectors	200 Hz BW
Surge bleed	15 Hz $\rightarrow$ 50 Hz, 30 %
Data filtering	4^{th} order Bessel
Electronic delay	about 4 msec

Table 1: Parameters on Caltech rig.

The air injectors are set at 27° to the axial direction opposite to the compressor rotor rotation. Experiments with the injector back pressure at 35 psig and 50 psig are carried out. The highest velocities of the air injected at 35 and 50 psig measured at the rotor face are approximately 23.6 and 30.2 m/sec respectively.

4. Results and Discussion

In this section, the results for the low and high B cases are presented. For the high B case, the results obtained via on-off and a simulated proportional axisymmetric air injection, as well as binary axisymmetric air injection for stall and a bleed valve for surge are compared.

4.1. Low B

Two cases with different injector back pressure at 35 psig and 50 psig are studied. A threshold for the stall amplitude, below which no control effort is commanded, is used. The closed-loop behavior of the system for the two cases are shown in Figure 6 with the hysteresis loops for the unactuated open-loop and with continuous air injection cases shown for comparison. Readers should note that the hysteresis loops overlap between the unactuated open-loop case and the case with 35 psig continuous air injection. Similar to the results reported in,[1] active control of stall is not achieved for the case where there is an overlapping region between the hysteresis loop for the unactuated open-loop case and the case with 35 psig continuous air injection. Control of stall is achieved for the 50 psig case where there is no overlap. A study is also performed using 60 psig injector back pressure and results are better than

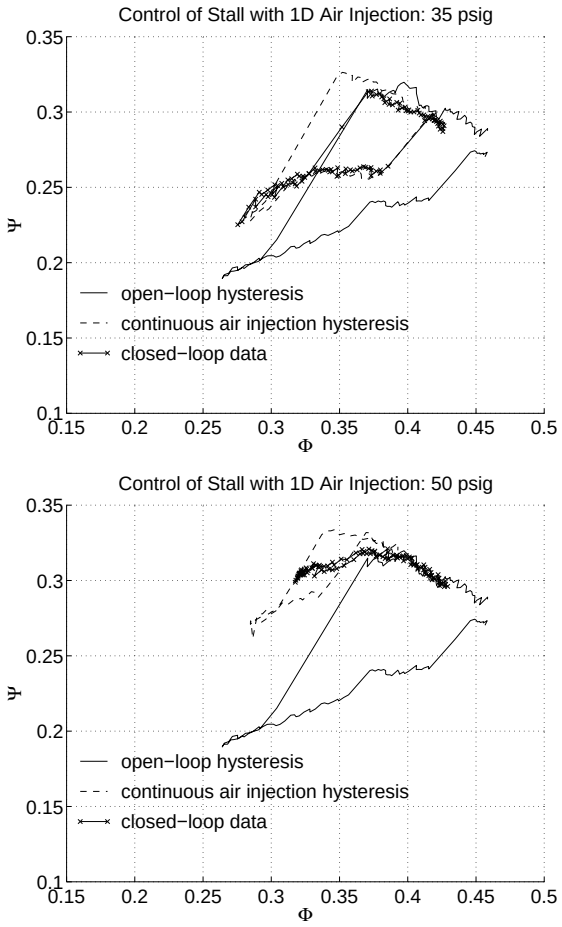

Figure. 6: Control of stall via binary 1D air injection on Caltech rig: 35 and 50 psig injector back pressure.

the 50 psig case.

Despite the observed evidence on the importance of overlapping of hystereses on control via axisymmetric air injection, the same conclusion is not at all clear from the model. When the control gain K in eq (2) is larger than $K_{\min}$ in eq (3), the criticality of the bifurcation is changed and the hysteresis loop is eliminated. Since K can be chosen arbitrarily large the nominal hysteresis loop can always be eliminated regardless of whether there is overlapping.

However, there is no account for actuation limits such as magnitude and rate saturations in the model. Due to noise on the experiment, a threshold on J below which control is not activated is implemented. This threshold, along with magnitude saturation, clearly limits the largest K that can be chosen since the largest gain becomes $1/J_{\text{thresh}}$. Also, bandwidth and rate limits on the actuation are essential in determining whether the control can "catch" the system, and are further constraints when coupled with

magnitude saturations.

For the results reported in this paper, the rate limit is conjectured to be the limiting factor in the overlapping hystereses case. When the system is operating at the stall inception point, the results of the actuation must be fast enough to trap the states of the system in the region of attraction of the controlled equilibrium. Otherwise the system stalls and the control is commanded to be fully on. And since the hystereses overlap, the system would remain stalled on the stalled branch of the actuated characteristic, and unstalls at the point of unstall of the actuated characteristic.

In the non-overlapping hystereses case, however, rate limit is *not* of importance. Since the hystereses do not overlap, the characteristic can be shifted *after* the system is stalled and the system will return to stall-free operation on the actuated characteristic. This is analogous to the case for bleed valve control in which the bleed valve magnitude limit is enough to clear the hysteresis loop.

Wang and Murray[10] presented a method of accounting for system and actuation limits on bleed valve control of stall via dynamical systems tools. Some preliminary work has been done to apply the technique to axisymmetric air injection control of stall.

4.2. High B

A combined algorithm of stall and surge control is implemented. The control law is of the form $u = KJ + \hat{K}\dot{\phi}$, proposed by Eveker et al.[5] The algorithm commands the injectors to inject air axisymmetrically when stall and/or surge is detected. For the case of 50 psig injector back pressure, the closed-loop system is stable without stall or surge. For the 35 psig case, the system stalls due to the inability of stall control. Figure 7 and 8 show the dynamic response of the system in the flow-pressure plane for 35 psig and 50 psig injector back pressure settings respectively.

A modification is made to simulate proportional injection. An upper and a lower limit on the first mode amplitude associated with pressure perturbation as well as $\dot{\phi}$ are introduced. The duty cycle of the injection mechanism is modified online according to the size of the detected stall and $\dot{\phi}$ amplitudes according to Table 2, with A_u and A_l representing the upper and lower limit of A, and $\dot{\phi}_u$ and $\dot{\phi}_l$ representing the upper and lower limit of $\dot{\phi}$ respectively.

Initial attempts in implementing the simulated proportional injection algorithm failed due to inappropriately chosen upper and lower limits for A and $\dot{\phi}$. After modifying the limits to significantly reduce the range of proportional control in A and $\dot{\phi}$ (essentially changing the gain), results similar to that shown in Figure 7 and 8 for 35 psig and 50 psig injector back pressure settings respectively are obtained. Figure 9 shows the dynamic data during closed-loop operation at surge inception point for 50 psig injector back pressure.

Control of stall using axisymmetric air injection and surge using a slow bleed valve (with a feedback on $\dot{\phi}$) is also implemented (Figure 10). A comparison of Figure 8 and 10 shows that the fluctuation in flow is greater while that in pressure is less in the latter case.

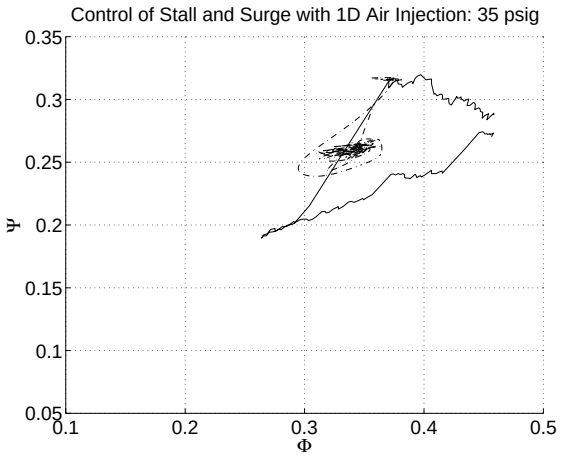

Figure. 7: Control of stall and surge via binary 1D air injection on Caltech rig: 35 psig injector back pressure. System stalls without surge.

duty cycle	condition
1	$(A > A_u) \mid (\dot{\phi} < \dot{\phi}_u)$
$\frac{A-A_l}{A_u-A_l} + \frac{\dot{\phi}-\dot{\phi}_u}{\dot{\phi}_l-\dot{\phi}_u}$	$(A_u > A > A_l)$ & $(\dot{\phi}_l > \dot{\phi} > \dot{\phi}_u)$
$\frac{A-A_l}{A_u-A_l}$	$(A_u > A > A_l)$ & $(\dot{\phi}_l < \dot{\phi})$
$\frac{\dot{\phi}-\dot{\phi}_u}{\dot{\phi}_l-\dot{\phi}_u}$	$(A < A_l)$ & $(\dot{\phi}_l > \dot{\phi} > \dot{\phi}_u)$
0	$(A < A_l)$ & $(\dot{\phi}_l < \dot{\phi})$

Table 2: Conditions for simulated proportional control.

5. Conclusion

Control of stall and surge is achieved on the Caltech rig with axisymmetric air injection. The injector back pressure are set at 35 psig and 50 psig as the cases studied. Control of stall in the low B

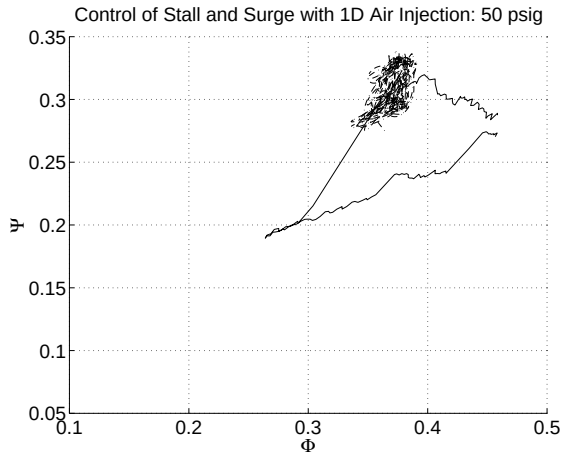

Figure. 8: Control of stall and surge via binary 1D air injection on Caltech rig: 50 psig injector back pressure.

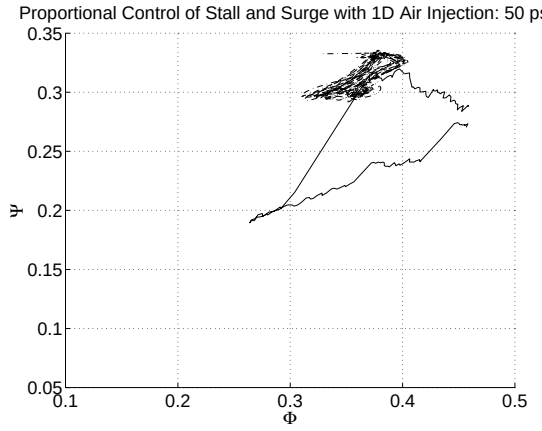

Figure. 9: Proportional control of stall and surge on Caltech rig: 50 psig injector back pressure.

case is achieved for 50 psig, but not 35 psig where the hysteresis loop of the unactuated open-loop case overlaps with that in the case with 35 psig continuous air injection. Simultaneous control of stall and surge in the high B case is again achieved in the 50 psig case only due to the inability of stall control in the 35 psig case.

A number of things are of future research interest. The experiments reported in this paper are carried out at a fixed physical location at two different injector back pressures. A full parametric study in terms of the axial, radial, and circumferential position of the injectors, and injector back pressure can identify the "optimal" axisymmetric air injection stall-surge controller. Evaluation of effects of bandwidth and rate limit of air injection on stall and surge control

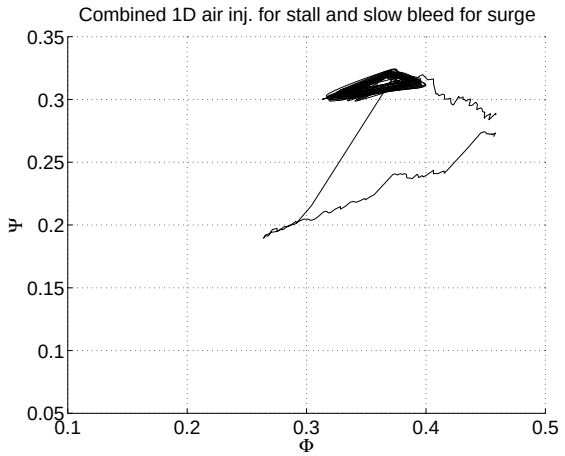

Figure. 10: Axisymmetric air injection for stall and bleed for surge on Caltech rig: 50 psig injector back pressure.

can also be studied. Given the possibility of stall and surge control with both bleed valves and air injection, various combinations of and trade-offs between the actuation mechanisms can be studied. This issue becomes particularly important in a multi-block model.

References

[1] R. L. Behnken. *Nonlinear Control and Modeling of Rotating Stall in an Axial Flow Compressor*. PhD thesis, California Institute of Technology, September 1996.

[2] R. L. Behnken and R. M. Murray. Combined Air Injection Control of Rotating Stall and Bleed Valve Control of Surge. In *Proceedings of American Control Conference*, pages 987–992, 1997.

[3] R. D'Andrea, R. L. Behnken, and R. M. Murray. Active Control of an Axial Flow Compressor via Pulsed Air Injection. *ASME Journal of Turbomachinery*, 119(4):742–752, 1998.

[4] I. J. Day. Active Suppression of Rotating Stall and Surge in Axial Compressors. *ASME Journal of Turbomachinery*, 115(1):40–47, 1993.

[5] K. M. Eveker, D. L. Gysling, and C. N. Nett. Integrated Control of Rotating Stall and Surge in Aeroengines. In *Proceedings of The International Society for Optical Engineering*, pages 21–35, April 1995.

[6] C. Freeman, A. G. Wilson, I. J. Day, and M. A. Swinbanks. Experiments in Active Control of Stall on an Aeroengine Gas Turbine. In *Proceedings of International Gas Turbine and Aeroengine Congress and Exhibition*, 1997. ASME 97-GT-280.

[7] D. L. Gysling and E. M. Greitzer. Dynamic Control of Rotating Stall in Axial-flow Compressors using Aeromechanical Feedback. *ASME Journal of Turbomachinery*, 117(3):307–319, 1995.

[8] F. E. McCaughan. Bifurcation Analysis of Axial Flow Compressor Stability. *SIAM Journal of Applied Mathematics*, 50(5):1232–1253, 1990.

[9] F. K. Moore and E. M. Greitzer. A Theory of Post-Stall Transients in Axial Compression Systems: Part 1–Development of Equations. *ASME Journal for Engineering for Power*, 108(1):68–78, 1986.

[10] Y. Wang and R. M. Murray. Effects of Noise, Magnitude Saturation and Rate Limits on Rotating Stall Control. In *Proceedings of Conference on Decision and Control*, pages 4682–4689, 1997.

[11] H. J. Weigl. Active Stabilization of Rotating Stall and Surge in a Transonic Single Stage Axial Compressor. Technical Report GTL 226, Massachusetts Institute of Technology, July 1997.

[12] H. J. Weigl, J. D. Paduano, L.G. Frechette, A. H. Epstein, and E. M. Greitzer. Active Stabilization of Rotating Stall in a Transonic Single Stage Axial Compressor. In *Proceedings of International Gas Turbine and Aeroengine Congress and Exhibition*, 1997. ASME 97-GT-411.

[13] S. Yeung and R. M. Murray. Nonlinear Control of Rotating Stall using 1-D Bleed Valve with Continuous Air Injection. In *Proceedings of Joint Propulsion Conference and Exhibit*, Seattle Washington, 1997. AIAA 97-2660.